The extraordinarily strong and cold polar vortex in the early northern winter 2015/16

V. Matthias,[1] A. Dörnbrack,[2] and G. Stober[1]

[1]Leibniz Institute of Atmospheric Physics

at the University of Rostock, Kühlungsborn,

Germany

[2]Institut für Physik der Atmosphäre,

DLR Oberpfaffenhofen, 82230

Oberpfaffenhofen, Germany

The Arctic polar vortex in the early winter 2015/16 was the strongest and coldest of the last 68 years. Using global reanalysis data, satellite observations, and mesospheric radar wind measurements over northern Scandinavia we investigate the characteristics of the early stage polar vortex and relate them to previous winters. We found a correlation between the planetary wave (PW) activity and the strength and temperature of the northern polar vortex in the stratosphere and mesosphere. In Nov/Dec 2015, a reduced PW generation in the troposphere and a stronger PW filtering in the troposphere and stratosphere, caused by stronger zonal winds in mid-latitudes, resulted in a stronger polar vortex. This effect was strengthened by the equatorward shift of PWs due to the strong zonal wind in polar latitudes resulting in a southward shift of the Eliassen-Palm flux divergence and hence inducing a decreased deceleration of the polar vortex by PWs.

Keypoints:

- formation of the coldest and strongest Arctic polar vortex in Nov/Dec 2015 for almost 70 years

- significant correlation of low polar vortex temperatures and weak stratospheric planetary wave activity

- mid-latitude stratospheric winds correlate with planetary wave activity and temperature in polar latitudes

1. Introduction

In northern hemispheric winters, the stratospheric polar vortex is usually disturbed by planetary waves (PWs). These disturbances manifest themselves in different kinds of stratospheric warmings occurring frequently during the Arctic winters. In early winter 2015/16, an extraordinarily strong and cold polar vortex formed. Strong and cold polar vortices are of special interest due to the possibility of the formation of wide-spread polar stratospheric clouds (PSCs) and the consequent depletion of ozone in spring [e.g. *WMO*, 2014]. In winter 2015/16 the stratosphere had the greatest potential yet seen for a massive Arctic ozone loss due to the record low temperatures in the lower stratosphere from December 2015 to February 2016 [*Manney and Lawrence*, 2016]. Here, we want to investigate the dynamical processes responsible for the particular dynamic evolution of the Arctic polar vortex in early winter 2015/16.

In the last three decades, unusually cold Arctic polar vortices were identified in early winters 1995/96, 1999/2000, 2002/03 and 2012/13 [*Manney and Sabutis*, 2000; *Sabutis and Manney*, 2000; *Manney et al.*, 2015]. *Manney and Sabutis* [2000] studied the development of the cold polar vortex of the early winter 1999/2000. *Sabutis and Manney* [2000] found that less wave activity was entering the upper stratosphere for a prolonged period, resulting in the low temperatures in this early winter. They identified the reduced wave propagation into mid- and high latitude upper stratosphere as the reason for the attenuated residual circulation resulting in a cold stratosphere. Based on these results *Sabutis and Manney* [2000] listed three factors necessary for producing an unusually cold Arctic polar vortex: i) less PW activity enters the stratosphere, ii) prolonged periods of small

PW activity, and iii) a background structure that prevents PW propagation into mid- and high latitude upper stratosphere. However, *Manney and Sabutis* [2000] stated that a reduced PW propagation can also occur in a weak polar vortex, when the temperature gradient between mid- and high latitudes is weak.

More recent studies of *Hinssen and Ambaum* [2010] show that 50% of the interannual variability of the northern hemispheric stratosphere is determined by variations in the 100 hPa eddy heat flux, a measure of the PWs energy entering the stratosphere [e.g., *Coy et al.*, 1997; *Pawson and Naujokat*, 1999; *Hinssen and Ambaum*, 2010]. *Newman et al.* [2001] found a positive correlation between the eddy heat flux at 100 hPa averaged between 45°N and 75°N and the polar cap temperature. *Polvani and Waugh* [2004] showed that weak eddy heat fluxes nearly always precede strong polar vortex events, which is consistent with wave-mean flow interaction theory [e.g. *Andrews et al.*, 1987].

In this paper, we investigate the early vortex evolution of the Arctic winter 2015/16 and intend to answer the following questions: What caused the strong and cold Arctic polar vortex in Nov/Dec 2015? In which way did the early stage of the Arctic polar vortex differ from previous winters? Was the excitation of PWs weaker in the troposphere? Were the stratospheric wind conditions suitable for vertically propagating PWs? In which way did the meridional position of the polar night jet influence the equatorward shift of PWs? For this purpose, we analyzed almost four decades of ERA-Interim data and seven decades of NCEP/NCAR data. To compare and extend the meteorological reanalysis, satellite and meteor radar data from Andenes (69°N, 16°E) are utilized. The paper is organized as follows: Section 2 gives an overview of the database and methods with an adjoining

presentation of our results in section 3. Conclusively, the results are discussed in section 4 and summarized in section 5.

2. Instruments and Database

To investigate the characteristics of the polar vortex, such as temperature, zonal wind and PW activity, we use the ERA-Interim reanalysis data [*Dee et al.*, 2011] with a horizontal resolution of 2° on 60 vertical model levels from 1000 to 1 hPa and with a temporal resolution of 6 hours. The data set includes 37 winters from Jan 1979 to Dec 2015. The ERA-Interim data set is in good agreement with other reanalyses in the lower stratosphere and with the Japanese 55-year Reanalysis in the upper stratosphere [*Simmons et al.*, 2014]. The agreement is even better in the Arctic than in the Antarctic [*Lawrence et al.*, 2015].

Addionally, we use the monthly means of the 68 year (1948 - present) long NCEP/NCAR reanalysis [*Kalnay et al.*, 1996] data set to show how extraordinarily cold and strong the polar vortex in Nov/Dec 2015 was.

For comparison and as an extension into the mesosphere we use temperature and geopotential height data from the Microwave Limb Sounder (MLS) onboard the Aura satellite [*Waters et al.*, 2006; *Livesey et al.*, 2015]. MLS has a global coverage from 82°S to 82°N on each orbit and a usable height range from approximately 11 to 97 km (261 - 0.001 hPa) with a vertical resolution of ∼4 km in the stratosphere and ∼14 km at the mesopause. The temporal resolution is one day at each location and data are available since Aug 2004 until today [*Livesey et al.*, 2015]. Note that version 4 MLS data was used and that the most recent recommended quality screening procedures of *Livesey et al.* [2015] have

been applied. To estimate the PW activity in the middle atmosphere, for one thing a two dimensional least-square method by *Wu et al.* [1995] is applied to the global data sets of ERA-Interim and MLS to obtain the quasi stationary PW1 amplitude, and for another thing the zonal mean is subtracted at each latitude to obtain the total eddy amplitude.

To investigate the vertical coupling by waves from the troposphere into the mesosphere, mesospheric wind data were used from a Meteor radar [*Hocking et al.*, 2001; *Stober et al.*, 2012] at Andenes (69°N,16°E) in northern Norway. The winds are available in a height range between 70 and 110 km with a vertical resolution of 2 km and a temporal resolution of one hour from 2003 until today. Background winds are obtained by fitting and subtracting the diurnal, semidiurnal and terdiurnal tides [e.g. *Pancheva et al.*, 2009].

Note that in all following correlation analyses a confidence level of 95% is used.

3. Results

Figure 1 shows the November/December means of the zonal mean tropospheric and stratospheric temperature profiles averaged between 60°N and 80°N from MLS (a), ERA-Interim (b) and NCEP/NCAR (d). The vertical temperature profiles of Nov/Dec 2015 (red) show distinct lower values compared to the ones of both data sets in all previous years. In the middle stratosphere between 20 and 30 km altitude, the mean temperatures of Nov/Dec 2015 are up to 4 K (MLS), 5 K (ERA-Interim) and 7 K (NCEP/NCAR) lower than the long-term average. The stratospheric temperatures beneath about 35 km altitude fall even below the standard deviations from the long-term average in all three data sets (Figs. 1a and b). The zonal mean zonal wind averaged between 60°N and 80°N as shown in Fig. 1c is distinctively stronger in Nov/Dec 2015 than in all other years and

exceeds the standard deviation by up to 15% in the altitude range from 20 km to 40 km. Accordingly, the results presented in Fig. 1 reveal an extraordinarily strong and cold Arctic polar vortex that formed in Nov/Dec 2015. Note that we define the strength of the polar vortex by the maximum zonal mean zonal wind averaged between 60°N and 80°N. The comparisons with the data from MLS, ERA-Interim and NCEP/NCAR highlight Nov/Dec 2015 as the strongest and coldest stratospheric vortex in the previous 68 years. In the following we investigate the causes for this extraordinarily strong and cold polar vortex in Nov/Dec 2015.

If the amplitude of a PW is large enough, it attenuates the residual meridional circulation, resulting in adiabatic heating in polar latitudes, i.e. warming the Arctic stratosphere [*Charney and Drazin*, 1961]. Figure 2 shows the amplitude of the stationary PW with wavenumber 1 (PW1) (a and b) and of the total eddy amplitude (c and d) each averaged between 60°N and 80°N from MLS and ERA-Interim. The correlation of the PW1 amplitude with the zonal mean temperature (red) and zonal wind (blue) in the same area is shown in Fig. 2e and 2f. The amplitude of the stationary PW1 in Nov/Dec 2015 (red line) is small compared to the other winters (grey lines) and below the standard deviation in both data sets. However, the winter 2013 had an even smaller PW1 amplitude than Nov/Dec 2015. Similar results are obtained for the total eddy amplitude (2c and d), which is much smaller in Nov/Dec 2015 than on the long term average. The average difference between the PW1 amplitude and the total eddy amplitude is ∼300 m for MLS and ∼150 m for ERA-Interim. Thus, on average the PW1 dominates the eddy field.

Both data sets show a positive and statistically significant correlation between the PW1 amplitude and the zonal mean temperature between about 20 and 50 km altitude (see Figs. 2e and f). The peak correlation coefficient in the shorter data set of MLS is 0.81 while it is 0.5 in the longer data set of ERA-Interim. There is a statistically significant negative correlation between the PW1 amplitude and the zonal wind in the stratosphere. Thus, the weaker the PW1 amplitude, the stronger and colder the stratospheric polar vortex. In the mesosphere, the correlation between PW1 amplitude and temperature is negative, i.e. the weaker the PW1 amplitude the warmer the mesospheric polar region. Note that this result is statistically significant in the lower mesosphere only. The anticorrelation of the mesospheric and stratospheric temperature in Arctic winter was already reported by *Cho et al.* [2004] using local temperature measurements at Resolute Bay (74°N, 94°W) and verified by *Siskind et al.* [2005] using global satellite observations.

Figure 1c reveals an exceptionally strong stratospheric zonal wind in Nov/Dec 2015. In order to investigate the vertical coupling in the middle atmosphere, Figure 3a depicts the observed zonal wind (tides removed) from 70 to 110 km altitude above Andenes, northern Norway (69°N,16°E) for the years 2003 to 2015. Generally the Nov/Dec tides-free mean zonal winds are weak and vary roughly between 5 and 10 m/s over the years. There is almost no vertical shear in this layer. The mean mesospheric wind in Nov/Dec 2015 was stronger compared to the previous years and also beyond the standard deviation from the mean. These findings indicate that strong stratospheric winds extend into the mesosphere.

To investigate the vertical coupling from the stratosphere into the mesosphere, Fig. 3b shows the correlation of the zonal wind at 84 km with the PW1 stratospheric amplitude

(black), temperature (red) and zonal wind (blue) each averaged between 60°N and 80°N. The mesospheric zonal wind is negatively correlated with the PW1 stratospheric amplitude and with the temperature showing a peak correlation coefficient of -0.82 for the PW1 amplitude and -0.73 for the temperature. There is also a positive correlation of 0.43 of the zonal wind at 84 km altitude and the stratospheric zonal mean zonal wind. Note that in contrast to the result from the PW1 amplitude temperature correlation, this value is statistically not significant. Nevertheless, the stronger zonal background wind in the mesosphere also reflects the weaker disturbances of the stratospheric polar vortex by the PW1. Thus, the weaker the PW1 amplitude in the polar stratosphere, the stronger the zonal wind in the mesosphere in Arctic polar latitudes. This result should be considered with caution since the local measurement can be within or outside of the polar vortex. Nevertheless, Andenes (69°N,16°E) is located in the middle of the latitude range (60°N – 80°N) considered here and is therefore suitable for an extension of our analysis into the mesosphere.

All the findings presented so far suggest that the formation of the strong and cold stratospheric Arctic polar vortex was maintained by weak stratospheric PW1 activity in Nov/Dec 2015. Hence, the following question arises: Why was the stratospheric PW activity so weak in Nov/Dec 2015 compared to the previous years? There are three possible mechanisms degrading the stratospheric PW activity: i) less formation of PWs in the troposphere ii) less vertical propagation of PWs from the troposphere into the stratosphere and iii) filtering of PWs in the lower stratosphere [e.g. *Sabutis and Manney*, 2000]. The vertical propagation of the stationary PW1 is only possible if the background

wind is larger than zero and not too strong [*Charney and Drazin*, 1961]. Therefore, we investigate in Fig. 4a and b the latitude-altitude cross-sections of the temperature and zonal wind anomalies in Nov/Dec 2015 from the climatological means. The stronger and colder Arctic polar vortex in Nov/Dec 2015 is visible in both images. Moreover, the tropical and subtropical troposphere exhibits a warm anomaly in Nov/Dec 2015. Thus, a stronger meridional temperature gradient between the tropics and polar latitudes existed compared to previous years. Due to the thermal wind relation, this leads to a stronger increase of the zonal wind with height from the troposphere to the stratosphere in mid-latitudes around 50°N that is visible in Fig. 4b. *Charney and Drazin* [1961] suggest that to strong zonal winds provide adverse conditions for vertical PW propagation. Figure 4c shows the correlation of the zonal mean zonal wind averaged between 40°N and 60°N and the PW1 amplitude (black) and temperature (red) averaged between 60°N and 80°N for Nov/Dec 2015, respectively. The polar PW1 amplitude and the temperature are significantly negatively correlated with the zonal wind in mid latitudes with peak values of -0.79 for the PW1 amplitude and -0.88 for the polar temperature. Thus, the stronger zonal wind in the troposphere and lower stratosphere in mid latitudes most probably provides adverse conditions for vertical propagation of PWs in the troposphere and lower stratosphere and a colder Arctic polar vortex.

The Eliassen-Palm flux divergence (EPD) represents the main forcing in the deceleration of the zonal wind in the northern hemispheric winter due to PWs [e.g. *Andrews et al.*, 1987]. The EPD of Nov/Dec 2015 (colored contours in Fig. 4d) is shifted southward and weakened compared to the climatological mean (black contour lines) in the troposphere

and stratosphere, confirming results of *Osprey et al.* [2016]. This weaker EPD results in a distinctive weaker deceleration of the zonal wind in the polar region.

The open question, whether there is a weaker PW generation in the troposphere or a stronger PW filtering on the way into the stratosphere, is investigated using the meridional eddy heat flux. Figure 5a shows the meridional eddy heat flux zonally averaged between 40°N and 60°N from ERA-Interim. Note that the eddy heat flux includes all waves and not only PW1. In Nov/Dec 2015 (red line), the eddy heat flux is small compared to the other winters (grey lines) and falls even below the standard deviation. Thus, PWs have a weaker amplitude in the troposphere and, hence, the PW activity is weaker in the stratosphere. Based on ERA-Interim the meridional heat flux at 100 hPa averaged for Nov/Dec is positively correlated with the temperature averaged between 60°N and 80°N (see Fig. 5b) ,which is consistent with *Newman et al.* [2001]. Thus we conclude that the attenuated PW activity in the stratosphere caused the cold Arctic polar vortex. This raises the question why the meridional heat flux was reduced? Figure 5b shows a statistically significant negative correlation between the meridional heat flux at 100 hPa and the meridional temperature gradient (red) in the troposphere with a peak value of -0.57. Thus, the stronger the meridional temperature gradient in the troposphere the weaker the PW activity in the troposphere and, hence, the weaker the PW activity in the stratosphere.

4. Discussion

There are different teleconnection patterns influencing the strength and temperature of the Arctic polar vortex [e.g. *Holton and Tan*, 1980; *Labitzke et al.*, 2002; *van Loon and*

Labitzke, 1987]. In the following we want to discuss the three most prominent teleconnections regarding the Arctic polar vortex in Nov/Dec 2015: the quasi-biennial oscillation (QBO), the solar cycle and El Niño.

In Fig. 4b a strong positive zonal wind anomaly strikes at the equator between 20 and 30 km indicating that the zonal wind is in its westerly phase of the QBO. *Holton and Tan* [1980] found a modulation of the mean zonal wind and PW activity in the northern winter stratosphere by the QBO, known as the Holton-Tan effect. Even though the mechanism is not fully understood until today, there is a consensus that during the easterly phase of the QBO the subtropical zero wind line reflects PWs poleward leading to a more disturbed polar vortex [e.g. *Holton and Tan*, 1980; *Anstey and Shepherd*, 2014; *Labitzke and Kunze*, 2009]. Commonly, the Holton-Tan effect starts in November in mid latitudes and peaks in December and January in mid and high latitudes [*Baldwin and Dunkerton*, 1998]. Since in Nov/Dec 2015 the QBO was in its westerly phase [e.g. *Osprey et al.*, 2016] the polar vortex is expected to be colder and stronger [e.g. *Holton and Tan*, 1980].

Labitzke et al. [2002] stated that besides the QBO phase, the solar cycle has an influence on the strength of the polar vortex. The early Arctic polar vortex tends to be colder and stronger during solar maximum than during solar minimum [*Labitzke et al.*, 2002]. In winter 2015/16 the solar radio flux amplitude was slightly lower compared to the last solar maximum but this was about 30% smaller compared to the three maxima before. Thus, there is no evidence for a dominant regime.

The warmer tropical and subtropical troposphere in Nov/Dec 2015 (see Fig. 4a) points to another powerful phenomenon occurring in the last winter: a remarkably strong El

Niño [*McPhaden et al.*, 2015]. The impact of the El Niño-Southern Oscillation (ENSO) on the stratospheric polar vortex is controversially discussed in many studies [e.g. *van Loon and Labitzke*, 1987; *Hamilton*, 1993; *Garfinkel and Hartmann*, 2007, 2008]. The consensus is that the mean winter (Dec, Jan, Feb) polar vortex is warmer and weaker during El Niño than during La Nina or the neutral ENSO phase [e.g. *Camp and Tung*, 2007; *Garfinkel and Hartmann*, 2008; *Graf and Zanchettin*, 2012]. This is caused by an increased PW1 amplitude during EL Niño [e.g. *Garfinkel and Hartmann*, 2008]. Another record El Niño occurred in winter 1997/98 [*Wolter and Timlin*, 1998]. The Arctic polar vortex of the early winter 1997 (see supplements) was warmer and weaker than the climatological mean, which is in contrast to Nov/Dec 2015 (see Fig. 4 a and b). Based on this comparison, one would suppose that the remarkably strong El Niño is not responsible for the extraordinary strong and cold Arctic polar vortex in Nov/Dec 2015. However, we found that the warmer tropical and subtropical troposphere, resulting in a stronger meridional temperature gradient, is responsible for the weaker planetary wave activity.

Summarizing, from the QBO phase we would expect a colder and stronger polar vortex in early winter 2015/16 but a warmer and weaker one from the record El Niño southern oscillation. The solar flux amplitude gives no evidence for an influence on the strength of the Arctic polar vortex. Thus the tropospheric processes leading to this extraordinarily cold and strong polar vortex in Nov/Dec 2015 are complex and need further investigations.

5. Conclusion

In this study, we investigated the characteristics and peculiarities of the extraordinarily strong and cold Arctic polar vortex in Nov/Dec 2015. For this purpose, 37 years of

ERA-interim data, 68 years of NCEP/NCAR data, 11 years of global satellite (MLS) observations, and 13 years of local radar measurements at Andenes (69°N, 16°E) in northern Norway were analyzed. The early winter Arctic stratosphere was the coldest in the last 37 years.

The extraordinarily strong and cold Arctic polar vortex in Nov/Dec 2015 was caused by a very low PW activity in the stratosphere, dominated by a weak PW1 amplitude. We hypothesize that the following sequence of processes is responsible for the weak PW activity in this early winter: the increased meridional temperature gradient in the troposphere induced a stronger vertical wind shear in mid latitudes due to the thermal wind balance. This stronger zonal wind in the troposphere and lower stratosphere adversely affected the vertical propagation of PWs [*Charney and Drazin*, 1961] as seen in the reduced meridional eddy heat flux. The weaker PW activity in the troposphere is responsible for the weaker PW activity in the stratosphere. This effect was amplified by the increased filtering of PWs in the stratosphere as seen in the reduced and southward shifted Eliassen-Palm flux divergence.

Possible influences of teleconnection patterns (QBO, solar cycle and El Niño) on the strength of the polar vortex were discussed. While from the QBO point of view a cold and strong Arctic polar vortex is expected, a warm and weak polar vortex is expected from the record strong El Niño.

References

Andrews, D. G., J. R. Holton, and C. B. Leovy (1987), *Middle atmosphere dynamics*, Academic Press.

Anstey, J. A., and T. G. Shepherd (2014), High-latitude influence of the quasi-biennial oscillation, *Quart. J. R. Met. Soc.*, *140*(678), 1–21, doi:10.1002/qj.2132.

Baldwin, M. P., and T. J. Dunkerton (1998), Quasi-biennial modulation of the southern hemisphere stratospheric polar vortex, *Geophys. Res. Lett.*, *25*(17), 3343–3346, doi:10.1029/98GL02445.

Camp, C. D., and K.-K. Tung (2007), Stratospheric polar warming by ENSO in winter: A statistical study, *Geophys. Res. Lett.*, *34*(4), n/a–n/a, doi:10.1029/2006GL028521, l04809.

Charney, J. G., and P. G. Drazin (1961), Propagation of planetary-scale disturbances from the lower into the upper atmosphere, *J. Geophys. Res.*, *66*(1), 83–109, doi:

10.1029/JZ066i001p00083.

Cho, Y.-M., G. G. Shepherd, Y.-I. Won, S. Sargoytchev, S. Brown, and B. Solheim (2004), MLT cooling during stratospheric warming events, *Geophys. Res. Lett.*, *31*(10), doi: 10.1029/2004GL019552, l10104.

Coy, L., E. R. Nash, and P. A. Newman (1997), Meteorology of the polar vortex: Spring 1997, *Geophys. Res. Lett.*, *24*(22), 2693–2696, doi:10.1029/97GL52832.

Dee, D. P., et al. (2011), The ERA-Interim reanalysis: configuration and performance of the data assimilation system, *Quart. J. R. Met. Soc.*, *137*(656), 553–597, doi: 10.1002/qj.828.

Garfinkel, C. I., and D. L. Hartmann (2007), Effects of the El NioSouthern Oscillation and the Quasi-Biennial Oscillation on polar temperatures in the stratosphere, *J. Geophys. Res.*, *112*(D19), n/a–n/a, doi:10.1029/2007JD008481, d19112.

Garfinkel, C. I., and D. L. Hartmann (2008), Different ENSO teleconnections and their effects on the stratospheric polar vortex, *J. Geophys. Res.*, *113*(D18), n/a–n/a, doi: 10.1029/2008JD009920, d18114.

Graf, H.-F., and D. Zanchettin (2012), Central pacific el nio, the subtropical bridge, and eurasian climate, *J. Geophys. Res.*, *117*(D1), n/a–n/a, doi:10.1029/2011JD016493, d01102.

Hamilton, K. (1993), An Examination of Observed Southern Oscillation Effects in the Northern Hemisphere Stratosphere, *J. Atmos. Sci.*, *50*(20), 3468–3474, doi: 10.1175/1520-0469(1993)050¡3468:AEOOSO¿2.0.CO;2.

Hinssen, Y. B. L., and M. H. P. Ambaum (2010), Relation between the 100-hpa heat flux and stratospheric potential vorticity, *J. Atmos. Sci.*, *67*(12), 4017–4027, doi: 10.1175/2010JAS3569.1.

Hocking, W., B. Fuller, and B. Vandepeer (2001), Real-time determination of meteor-related parameters utilizing modern digital technology, *J. Atmos. Solar-Terr. Phys.*, *63*(2-3), 155 – 169.

Holton, J. R., and H.-C. Tan (1980), The Influence of the Equatorial Quasi-Biennial Oscillation on the Global Circulation at 50 mb, *J. Atmos. Sci.*, *37*(10), 2200 – 2208, doi:10.1175/1520-0469(1980)037<2200:TIOTEQ>2.0.CO;2.

Kalnay, E., et al. (1996), The NCEP/NCAR 40-Year Reanalysis Project, *Bull. Amer. Meteorol. Soc.*, *77*(3), 437–471, doi:10.1175/1520-0477(1996)077¡0437:TNYRP¿2.0.CO;2.

Labitzke, K., and M. Kunze (2009), On the remarkable Arctic winter in 2008/2009, *J. Geophys. Res.*, *114*(D1), doi:10.1029/2009JD012273.

Labitzke, K., J. Austin, N. Butchart, J. Knight, M. Takahashi, M. Nakamoto, T. Nagashima, J. Haigh, and V. Williams (2002), The global signal of the 11-year solar cycle in the stratosphere: observations and models, *J. Atmos. Solar-Terr. Phys.*, *64*(2), 203 – 210, doi:http://dx.doi.org/10.1016/S1364-6826(01)00084-0.

Lawrence, Z. D., G. L. Manney, K. Minschwaner, M. L. Santee, and A. Lambert (2015), Comparisons of polar processing diagnostics from 34 years of the ERA-Interim and MERRA reanalyses, *Atmos. Chem. Phys.*, *15*(7), 3873–3892, doi:10.5194/acp-15-3873-2015.

Livesey, N. J., et al. (2015), EOS MLS Version 4.2x level 2 data quality and description document, *Jet Propulsion Laboratory, California Institute of Technology, Pasadena, CA.*

Manney, G. L., and Z. D. Lawrence (2016), The major stratospheric final warming in 2016: Dispersal of vortex air and termination of arctic chemical ozone loss, *Atmos. Chem. Phys. Discuss.*, *2016*, 1–40, doi:10.5194/acp-2016-633.

Manney, G. L., and J. L. Sabutis (2000), Development of the polar vortex in the 19992000 arctic winter stratosphere, *Geophysical Research Letters*, *27*(17), 2589–2592, doi:10.1029/2000GL011703.

Manney, G. L., Z. D. Lawrence, M. L. Santee, N. J. Livesey, A. Lambert, and M. C. Pitts (2015), Polar processing in a split vortex: Arctic ozone loss in early winter 2012/2013, *Atmos. Chem. Phys.*, *15*(10), 5381–5403, doi:10.5194/acp-15-5381-2015.

McPhaden, M. J., A. Timmermann, M. J. Widlansky, M. A. Balmaseda, and T. N. Stockdale (2015), The Curious Case of the EL Nino That Never Happened: A Perspective from 40 Years of Progress in Climate Research and Forecasting, *Bull. Amer. Meteorol. Soc.*, *96*(10), 1647–1665, doi:10.1175/BAMS-D-14-00089.1.

Newman, P. A., E. R. Nash, and J. E. Rosenfield (2001), What controls the temperature of the arctic stratosphere during the spring?, *J. Geophys. Res.*, *106*(D17), 19,999–20,010, doi:10.1029/2000JD000061.

Osprey, S. M., N. Butchart, J. R. Knight, A. A. Scaife, K. Hamilton, J. A. Anstey, V. Schenzinger, and C. Zhang (2016), An unexpected disruption of the atmospheric quasi-biennial oscillation, *Science*, doi:10.1126/science.aah4156.

Pancheva, D., R. Mukhtarov, B. Andonov, N. J. Mitchell, and J. M. Forbes (2009), Planetary waves observed by TIMED/SABER in coupling the stratosphere-mesosphere-lower thermosphere during the winter of 2003/2004: Part 1–Comparison with the UKMO temperature results, *J. Atmos. Solar-Terr. Phys.*, *71*(1), 61 – 74, doi: 10.1016/j.jastp.2008.09.016.

Pawson, S., and B. Naujokat (1999), The cold winters of the middle 1990s in the northern lower stratosphere, *J. Geophys. Res.*, *104*(D12), 14,209–14,222, doi: 10.1029/1999JD900211.

Polvani, L. M., and D. W. Waugh (2004), Upward Wave Activity Flux as a Precursor to Extreme Stratospheric Events and Subsequent Anomalous Surface Weather Regimes, *J. Climate*, *17*(18, 0894-8755), 3548 – 3554, doi:10.1175/1520-0442(2004)017¡3548:UWAFAA¿2.0.CO;2.

Sabutis, J. L., and G. L. Manney (2000), Wave propagation in the 19992000 arctic early winter stratosphere, *Geophys. Res. Lett.*, *27*(19), 3205–3208, doi: 10.1029/2000GL011767.

Simmons, A. J., P. Poli, D. P. Dee, P. Berrisford, H. Hersbach, S. Kobayashi, and C. Peubey (2014), Estimating low-frequency variability and trends in atmospheric temperature using ERA-Interim, *Quart. J. R. Met. Soc.*, *140*(679), 329–353, doi: 10.1002/qj.2317.

Siskind, D. E., L. Coy, and P. Espy (2005), Observations of stratospheric warmings and mesospheric coolings by the TIMED SABER instrument, *Geophys. Res. Lett.*, *32*(9), doi:10.1029/2005GL022399, l09804.

Stober, G., C. Jacobi, V. Matthias, P. Hoffmann, and M. Gerding (2012), Neutral air density variations during strong planetary wave activity in the mesopause region derived from meteor radar observations, *J. Atmos. Solar-Terr. Phys.*, *74*(0), 55 – 63, doi:10.1016/j.jastp.2011.10.007.

van Loon, H., and K. Labitzke (1987), The southern oscillation. part v: The anomalies in the lower stratosphere of the northern hemisphere in winter and a comparison with the quasi-biennial oscillation, *Mon. Weather Rev.*, *115*(2), 357–369, doi:10.1175/1520-0493(1987)115¡0357:TSOPVT¿2.0.CO;2.

Waters, J. W., et al. (2006), The Earth Observing System Microwave Limb Sounder (EOS MLS) on the Aura Satellite, *IEEE Transactions on Geoscience and Remote Sensing*, *44*(5), 1075–1092, doi:10.1109/TGRS.2006.873771.

WMO (2014), Scientific assemssment of ozone depletion: 2014, global Ozone Res. and Monit. Prj. Rep. 55. Geneva, Switzerland.

Wolter, K., and M. S. Timlin (1998), Measuring the strength of ENSO events: How does 1997/98 rank?, *Weather*, *53*(9), 315–324, doi:10.1002/j.1477-8696.1998.tb06408.x.

Wu, D. L., P. B. Hays, and W. R. Skinner (1995), A Least Squares Method for Spectral Analysis of Space-Time Series, *J. Atmos. Sci.*, *52*(20), 3501–3511, doi:10.1175/1520-0469(1995)052¡3501:ALSMFS¿2.0.CO;2.
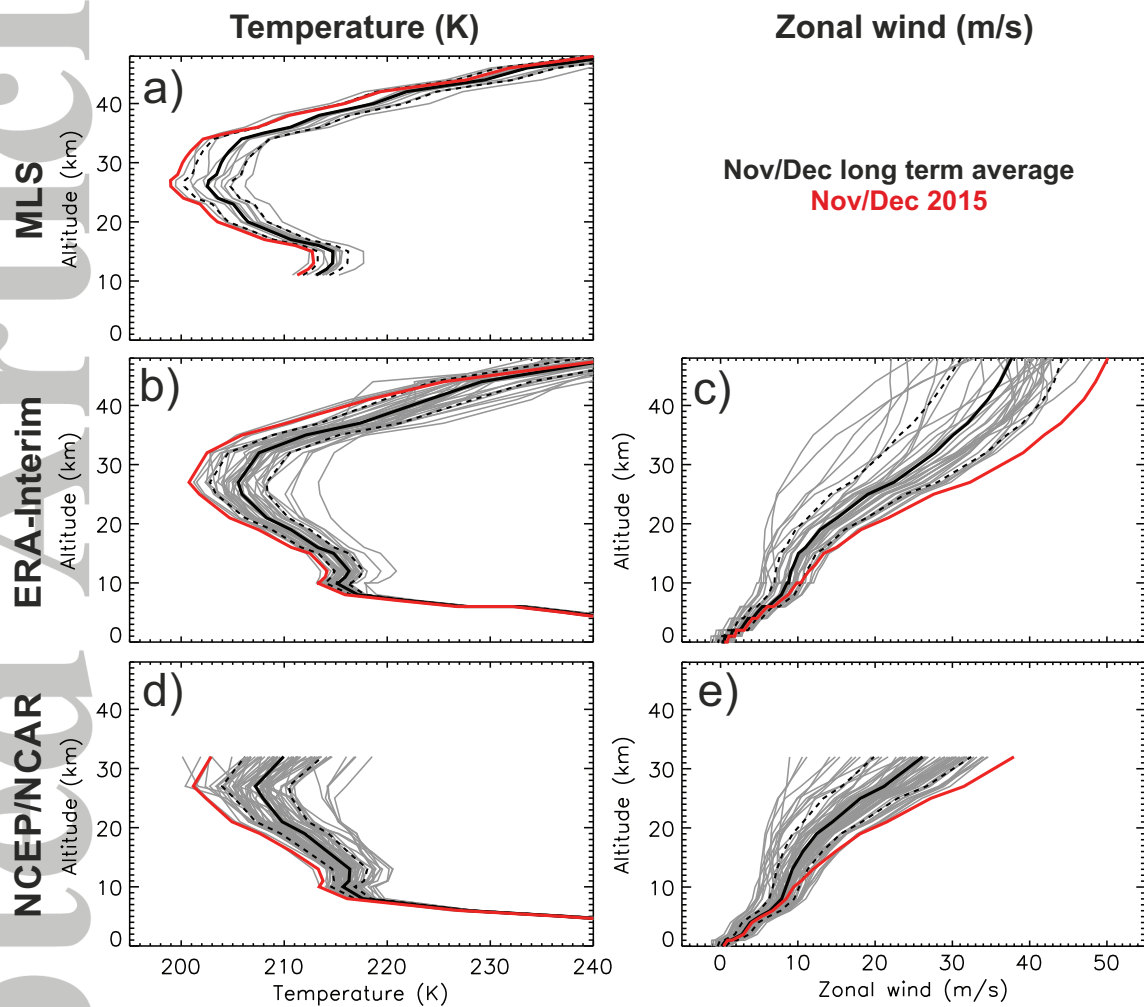
Figure 1. Vertical profiles of the Nov/Dec mean of zonal mean temperature (a, b) and zonal wind (c) averaged between 60°N and 80°N from MLS (a), ERA-Interim (b, c) and NCEP/NCAR (d, e). Thin grey lines represent the means from the available years (MLS = 12, ERA-Interim = 37, NCEP/NCAR=68). Solid black lines are the long-term averages. Their respective standard deviations are plotted as dashed lines. The red lines represent the Nov/Dec 2015 means.
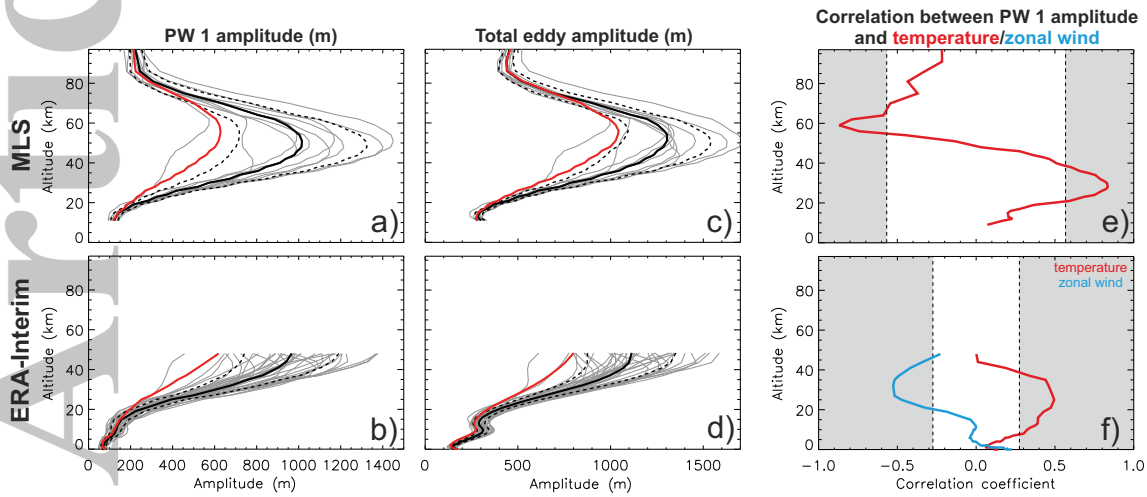
Figure 2. Vertical profiles of the Nov/Dec mean of PW1 amplitude (a and b) and total eddy amplitude (c and d) averaged between 60°N and 80°N from MLS and ERA-Interim. Thin grey lines represent the means from the available years (MLS = 12, ERA-Interim = 37). Solid black lines are the long-term averages. Their respective standard deviations are plotted by dashed lines. The red lines represent Nov/Dec 2015. Note that the total eddy heat flux includes all waves, i.e. traveling and stationary waves. e) and f): Correlation coefficient between the PW1 amplitude and the zonal mean temperature (red) and zonal wind (blue) averaged between 60°N and 80°N from MLS and ERA-Interim. The grey-shaded areas depict the range of statistically significant correlation coefficients.
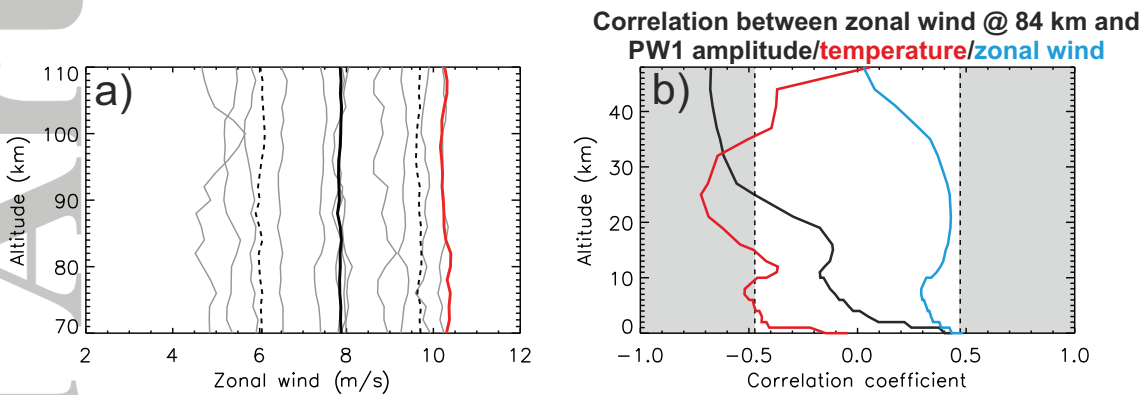
Figure 3. (a):Vertical profiles of the Nov/Dec mean of the zonal wind at Andenes (69°N, 16°E) determined from the Meteor radar for the years 2003 to 2015 (thin gray lines). The solid black line shows the long-term average, its standard deviation is plotted by dashed lines. The red line represents Nov/Dec 2015. (b): Correlation coefficients between the zonal wind at 84 km altitude from radar data and: PW1 amplitude (black); temperature (red) and zonal mean zonal wind (blue) averaged between 60°N and 80°N from ERA-Interim data.
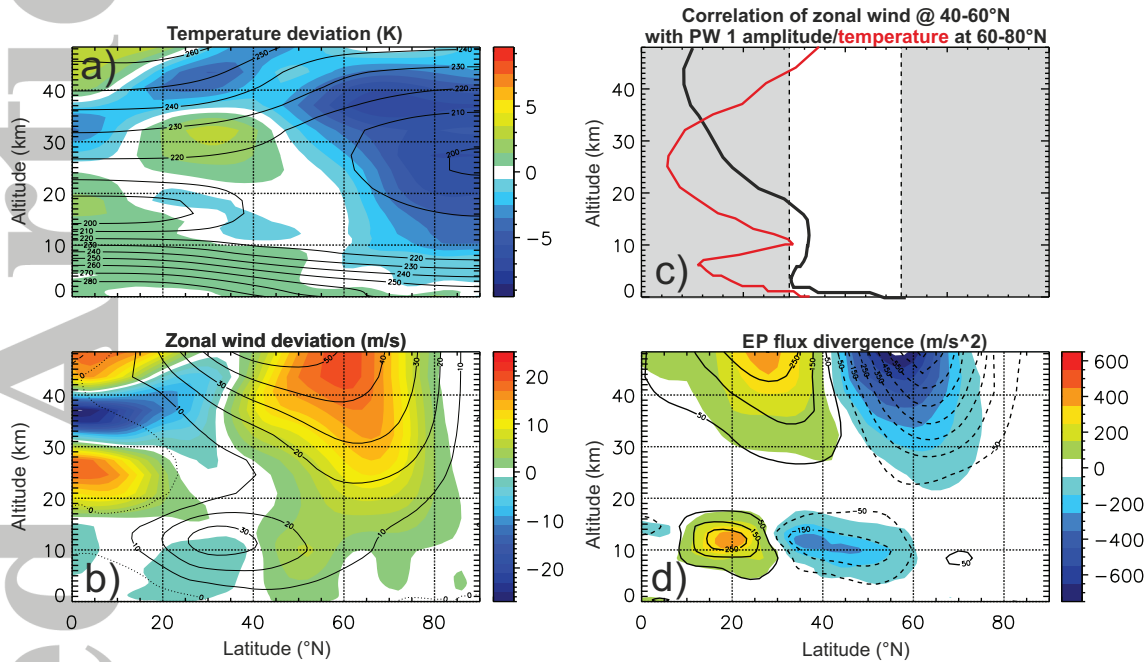
Figure 4. Latitude-height cross-sections of the Nov/Dec 2015 anomalies from the long term mean of zonal mean temperature (a) and zonal wind (b) from ERA-Interim data. (c): Correlation coefficient between zonal mean zonal wind averaged between 40° and 60°N and: PW1 amplitude (black); temperature (red) averaged between 60°N and 80°N from ERA-Interim. (d): Latitude-height cross-section of the Eliassen-Palm flux divergence of the Nov/Dec mean for 2015 (colored contour) and for the climatological mean (black contour lines).
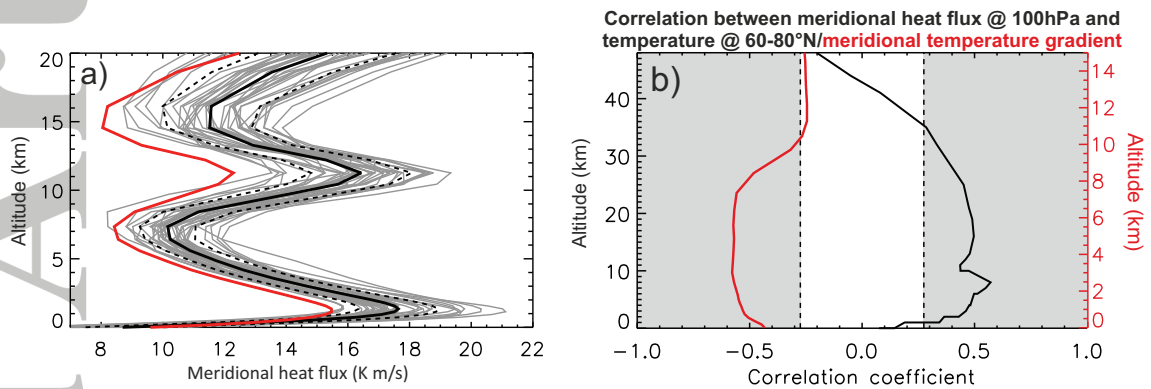
Figure 5. (a): Vertical profiles of the Nov/Dec mean of eddy heat flux averaged between 40°N and 60°N from ERA-Interim data. Black contour lines represent the climatological mean. (b): Correlation coefficient between the meridional heat flux at 100 hPa averaged between 40°N and 60°N and: temperature averaged between 60°N and 80°N from ERA-Interim (black); meridional temperature gradient between the equator and 80°N (red). The grey-shaded areas depict the range of statistically significant correlation coefficients.